IMPROVED SURFACE-WAVE DISPERSION MODELS, AMPLITUDE MEASUREMENTS, AND AZIMUTH ESTIMATES

Jeffry L. Stevens, David A. Adams, G. Eli Baker, Mariana G. Eneva and Heming Xu

Science Applications International Corporation

Sponsored by Air Force Research Laboratory

Contract No. DTRA01-01-C-0082

ABSTRACT

Surface waves are of primary importance for nuclear monitoring because the Ms:mb discriminant and its regional variants are among the most reliable means of determining whether an event is an earthquake or an explosion. The primary goal of this project is to reduce the magnitude threshold for which surface waves can be identified and measured reliably and to improve the accuracy of surface wave measurement, using phase-matched filtering and global regionalized earth and dispersion models.

This is the final year of a three-year project. Following are the most significant products and results of this work:

(1) Assembled a dataset of dispersion measurements of over one million data points. Some of this dataset came from our own measurements, but most came from other research studies, and we thank all of those scientists who have contributed to this effort. This dataset is one of the largest dispersion datasets ever assembled and is particularly unique in its coverage for a broad range of frequencies.

(2) Developed and have continuously improved a set of global earth models and dispersion models defined on a one-degree grid. These models were developed by simultaneously inverting the entire dataset for a set of earth structures, which in turn allow surface wave dispersion to be calculated between any two points on the earth at any set of frequencies, with the dispersion models constrained by the large dataset. These global earth and dispersion models are available on request to other researchers working in this program.

(3) Implemented the azimuth-estimation technique developed by Selby using Chael's algorithm, tested it on a large dataset of the International Monitoring System (IMS) data, and demonstrated that it is a major improvement over other commonly used azimuth-estimation techniques. This azimuth-estimation technique can be used together with the existing detection test based on consistency of measurement with surface-wave-dispersion maps, to reduce the detection threshold for which surface waves can be reliably identified and measured.

(4) Implemented and tested a path-corrected spectral magnitude, developed procedures for optimizing it and evaluated the discrimination capability of this and other types of surface wave measurements. Two particularly important results of this work are (a) the path-corrected spectral magnitude is independent of distance and unaffected by dispersion and therefore can be measured at any distance, including very close to the source, and it will have the same value as a measurement made at a greater distance. The path-corrected spectral magnitude is therefore a "regional Ms" which has been a long-term goal of this program (b) for discrimination purposes, surface waves should be measured at periods greater than 10 seconds. Periods of 10 seconds and longer can be measured even at very close range, and there is only a small S/N improvement, if any, at shorter periods. Any benefit from measurement at higher frequencies is lost due to the decrease in earthquake spectral amplitude relative to explosions at higher frequencies.

(5) Performed a study of "problem cases," where surface wave dispersion and/or amplitudes are inconsistent with model predictions. Typically, these cases occur where there are strong heterogeneities in earth structure along the path, particularly for grazing incidence along large changes in material properties. Ray theory predicts that surface waves will take the minimum time path between the source and receiver in such cases, but the observed waveforms are considerably more complex than this. In cases of large-velocity contrast such as the Tarim Basin region, there are multiple surface wave arrivals with a distinct arrival passing through the basin and another traveling around it. The arrivals merge at longer periods. Special care is required for construction and use of dispersion and attenuation models in such cases.

OBJECTIVE

The goal of this project is to reduce the magnitude threshold for which surface waves can be identified and measured reliably and to improve the accuracy of surface wave measurement, using phase-matched filtering, development of global regionalized earth and dispersion models, and other techniques.

RESEARCH ACCOMPLISHED

Overview

The importance of long period (>~10 second) surface waves for nuclear monitoring is in the discrimination capability of the M_s:m_b discriminant and its variants (Marshall and Basham, 1972; Stevens and Day, 1985). In general, contained underground explosions generate larger m_b relative to M_s than earthquakes of comparable size. This is one of the most reliable discriminants, but it has a few limitations:

1. Body waves can be measured for significantly smaller events than surface waves, so the discriminant is not useful for very small events. In this project we have addressed this issue by investigating methods to reduce the threshold for which surface waves can be reliably identified and measured, including the development of improved dispersion maps constrained by a very large data set to facilitate phase-matched filtering.

2. Although the strongest surface wave signals are at the closest distances, M_s is an unreliable amplitude measure at regional and local distances because of differences in dispersion and variations in the frequency content of the signal. We have addressed this issue by developing surface wave measurement techniques that can be used at local and regional distances, even very close to the source, which are consistent with measurements made at greater distances.

3. The discrimination capability of surface waves decreases with increasing frequency because the spectral difference between earthquakes and explosions declines. We have addressed this issue by analyzing surface wave and noise measurements to define the optimum frequency bands for discrimination.

4. Incorrect association of surface waves with the wrong event is a problem that can potentially lead to misclassification of an explosion as an earthquake. We have addressed this issue in two ways: first, by improving dispersion models that are used in the dispersion test for surface wave identification; and second by implementing and testing an improved azimuth estimation technique that can be used to improve association of surface waves with the corresponding event.

5. In general, surface waves can be modeled quite well using path-averaged dispersion and attenuation calculated from discrete plane-layered earth models and great circle propagation; however, there are some complex cases where standard methods of measuring surface wave dispersion and amplitude measurement do not work well. We have investigated some problem cases and made some suggestions for techniques to handle these situations.

Dispersion data set

We have been developing global, regionalized dispersion models that allow the phase and group velocity to be calculated between any two points on the earth. We have done this by accumulating a very large data set of dispersion measurements derived by a number of researchers, and then inverting this data set to determine earth structure, which in turn is used to generate phase and group velocity maps at all frequencies. The data set now contains more than one million data points. The dispersion data set has been derived from a variety of regional and global studies, including the following: global surface wave-group velocities from earthquakes derived using IMS data (Stevens and McLaughlin, 1996), as well as our own measurements derived from IMS data and several other data sets; surface-wave phase and group-velocity dispersion curves from underground nuclear test sites (Stevens, 1986; Stevens and McLaughlin, 1988), calculated from earth models for 270 paths (test site—station combinations) at 10 frequencies between 0.015 and 0.06 Hz; phase and group-velocity measurements for western Asia and Saudi Arabia from Mitchell et al.(1996) for 12 paths at 17 frequencies between 0.012 and 0.14 Hz; the global phase-velocity model of Ekstrom et al. (1996) for 9 periods between 35 and 150 seconds calculated for each grid block from a spherical harmonic expansion of order l = 40; group velocity measurements for Eurasia from Ritzwoller et al.

(1996) and Levshin et al.(1996) for 20 frequencies between 0.004 and 0.1 Hz with 500 to 5,000 paths per frequency; Antarctic and South American group velocity measurements from the University of Colorado (Vdovin et al., 1999; Ritzwoller et al., 1999); high-frequency Eurasian dispersion measurements from the University of Colorado (Levshin et al. 2003), a large set of dispersion measurements from Saudi Arabia provided by Herrmann and Mokhtar at St. Louis University; a data set from Los Alamos National Laboratory (Yang et al. 2002) for 2000 individual paths from Central Asia ranging between 0.05 Hz and 0.23 Hz, and a data set developed by Huang et al. (2003) for 9,730 paths from China. Considerable quality control was performed on the data set, and questionable data were removed or downweighed. Some of the data were improved substantially by relocating events from their original locations to the improved locations of Engdahl et al. (1998). The distribution of the group velocity data set at periods of 50, 20, and 10 seconds is illustrated in Figure 1.

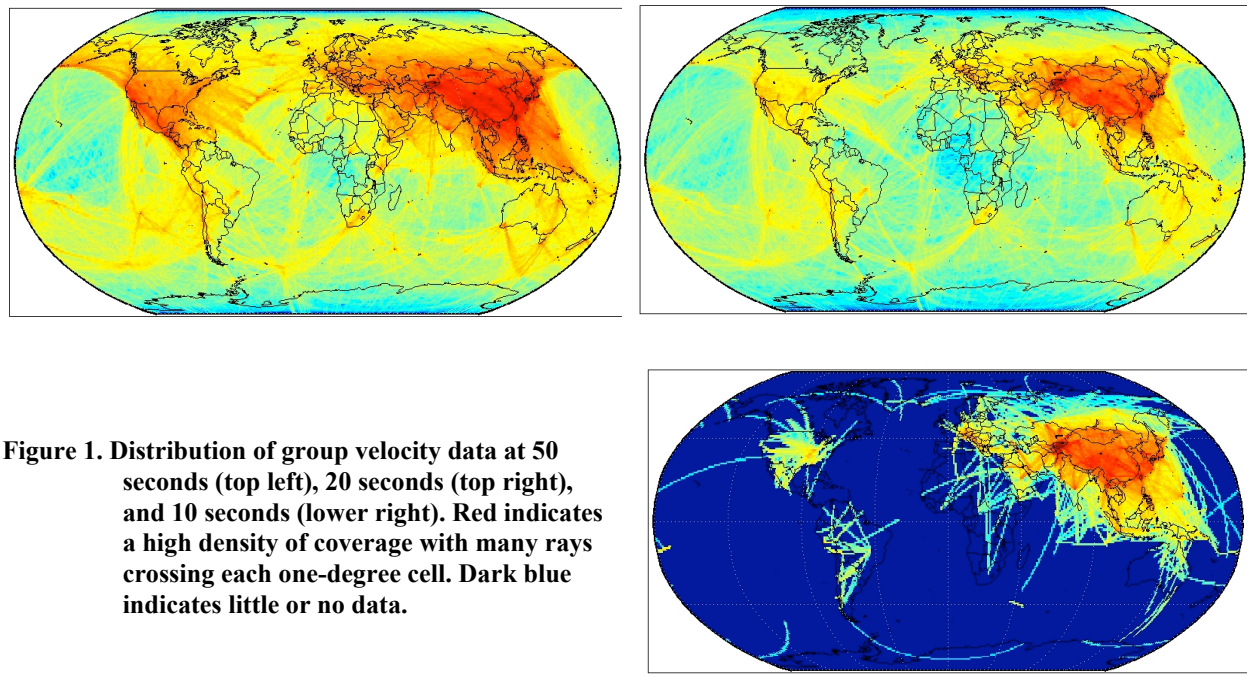

Figure 1. Distribution of group velocity data at 50 seconds (top left), 20 seconds (top right), and 10 seconds (lower right). Red indicates a high density of coverage with many rays crossing each one-degree cell. Dark blue indicates little or no data.

Global earth models and dispersion models

By developing dispersion maps based on earth models, we are able to invert all relevant data in a single inversion. The data include phase-velocity and group-velocity measurements measured along specific paths at all frequencies, as well as some phase and group velocity data points derived from models (e.g., the Harvard-phase velocity models). Developing dispersion maps based on earth models has some additional advantages relative to the more common technique of performing tomographic inversions separately for each frequency. In particular, we can easily include information from other studies leading to physically reasonable constraints on dispersion. For our earth models this information consists of the boundaries between geologic zones, bathymetry of oceans, thicknesses of sediments and ice, Moho depths, and previous estimates of seismic velocities derived from existing earth models. The regionalized earth model consists of 1º x 1º blocks and is made up of layers of ice, water, sediments, crust, and upper mantle. Currently this model depends on 9,008 free parameters that are adjusted by a damped least-squares fit to Rayleigh wave-dispersion data. The free parameters are the S-wave velocities of layers of 577 different model types. Other constrained parameters in the model are P-wave velocities, densities, and Q. The model types are based on the Crust 2.0 2º x 2º crustal types (Bassin et al., 2000 and Laske et al. 2001) and also on ocean ages (Stevens and Adams, 2000). The top few km of the model (consisting of water, ice and/or sediments) are fixed and match data from one degree bathymetry maps made by averaging Etopo5 five-minute measurements of topography, and Laske and Masters (1997) one-degree maps of sediments. There is an explicit discontinuity between the bottom of the sediments and the crust. There are three or more crustal layers. The Crust 2.0 models, which were the starting point for these structures, have three crustal layers, but we found it necessary to add more layers in regions of thick crust.

There is another explicit discontinuity at the Crust/Mantle boundary. The Moho depth is derived from Crust 2.0 and varies on a 2º grid. The mantle starting model is derived from AK135 (Kennett, et al, 1995). With these constraints, the inversion is performed for the shear velocity of the crust and upper mantle to a depth of 300 km. Below 300 km the earth structure is fixed, and the inversion model is required to be continuous with the mantle structure at the base of the inversion. In broad ocean areas, we replace the Crust 2.0 model with models distinct for each ocean and subdivided by ocean age. We also separate into distinct models Crust 2.0 models that are geographically separated. So, for example, if Crust 2.0 has the same model type in North America and in Asia, we use the same starting model for each, but treat them as separate models in the inversion.

The inversion procedure for the 3D earth model

The relationship between dispersion and the shear wave velocities of the layers in the earth model is nonlinear, so the shear velocities are estimated by an iterative least-squares inversion procedure. At each step a system of tomographic equations is formed, augmented by additional equations of constraint, and then solved by the LSQR algorithm. The equations solved are

$$\begin{bmatrix} A \\ sH \\ \lambda I \end{bmatrix} \vec{\Delta x} = \begin{bmatrix} \vec{\Delta d} \\ -sH\vec{x} \\ \lambda\left(\vec{x}_c - \vec{x}\right) \end{bmatrix} + \vec{\varepsilon}\,, \tag{1}$$

where Δx is the vector of adjustments to the shear wave slownesses of layers in each of the 577 model types. Δd is the vector of slowness differences between predicted and observed dispersion measurements. ε is the vector of residuals that remain after inversion (the inversion minimizes $|\varepsilon|$). x is the vector of slownesses estimated in the previous iteration. The elements of the matrix A consist of partial derivatives of dispersion predictions with respect to shear wave slownesses in each layer. H is a difference operator that applies to vertically neighboring layers and has the effect of constraining the vertical smoothness of velocity profile. H applies to layers in the crust and upper mantle, but has explicit discontinuities at the crust/mantle boundary and at the base of surface sediments. s is the weighting of the smoothness constraint and can be a diagonal matrix (for variably weighted smoothing) or a scalar (constant smoothing). A different smoothing parameter can be selected for each model type. Lateral smoothing, which is usually applied in tomography studies, is executed indirectly in our study through the selection of the model types. I is the identity matrix and λ weighs the damping, which constrains the norm of the difference between final slownesses and constraining model slownesses x_c (in this case, a variant of the Crust 2.0 values). The variable λ can be a scalar for constant damping, or a diagonal matrix for variable damping. As with smoothing, variable damping is implemented so that a different parameter can be selected for each model type.

The Selby/Chael algorithm for azimuth estimation

This section summarizes work done under this project that is described in more detail by Baker and Stevens (2004).

As part of its responsibilities under the Comprehensive Nuclear-Test-Ban Treaty (CTBT), the International Data Center (IDC) automatically processes seismic data recorded at IMS stations, identifying surface waves and measuring surface wave amplitude and M_s (Stevens and McLaughlin, 2001). Three-component backazimuth estimates derived using the current, spectral methods are recorded but are too inaccurate to use for association. That method is based on an algorithm originally proposed (Smart, 1978) as part of a surface wave detector, rather than as a means of estimating the backazimuth. Selby (2001) suggested that another detection technique (Chael, 1997), based on cross-correlation of the vertical and Hilbert transformed radial component Rayleigh wave records, could be used for backazimuth estimation and would improve IDC processing.

To compare the performance of the algorithms, we incorporated the Chael/Selby (CS) algorithm into the automatic surface-wave processing software that uses the current IDC method (CM). Under current IDC procedures, for an event location and time based on body-wave arrivals, a surface wave is considered detected if it passes a dispersion test in the group velocity window predicted for the event. We tested both algorithms on 2,599 records that passed the dispersion test and 2,363 generally poorer S/N records that failed, all from events that had at least four surface-wave detections. We assessed the performance of each algorithm for different passbands and group velocity windows.

Figure 2 shows histograms of backazimuth residuals for the CM and one implementation of the CS algorithm for a frequency band of 0.3–0.5 Hz. The CS algorithm performs better in two ways. First, the CM applied as it is currently used in the automatic processing, has errors of 180° for a significant number of events. This is due to the 180-degree ambiguity in Love wave polarization, which causes large Love wave amplitudes to increase the likelihood of a 180-degree error in backazimuth. Second, the histograms reveal many more outliers for the CM than for the CS algorithm.

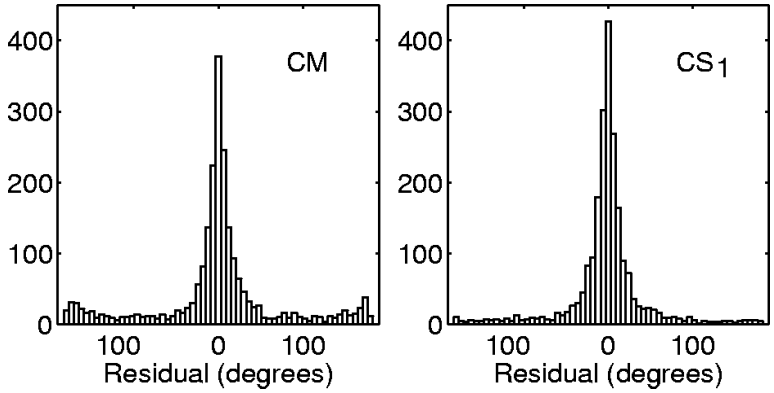

Figure 2. Backazimuth residuals for 0.03–0.05 Hz using the current method (left) and the Chael/ Selby algorithm.

Figure 3 shows the backazimuth residuals for each of the algorithms vs event size, which serves as a proxy for the signal-to-noise ratio. For large events, the CM's performance is almost comparable to the CS algorithms, except for a large number of sign errors. The greatest advantage of the CS algorithm is in estimating backazimuth of smaller events, especially at lower frequency, where the CM fails badly. We use the scaled-median absolute deviation (SMAD), the one-norm measure of the central tendency, to provide a measure of the spread of data about the central value that is less biased by outliers than the STD in heavy-tailed data such as these.

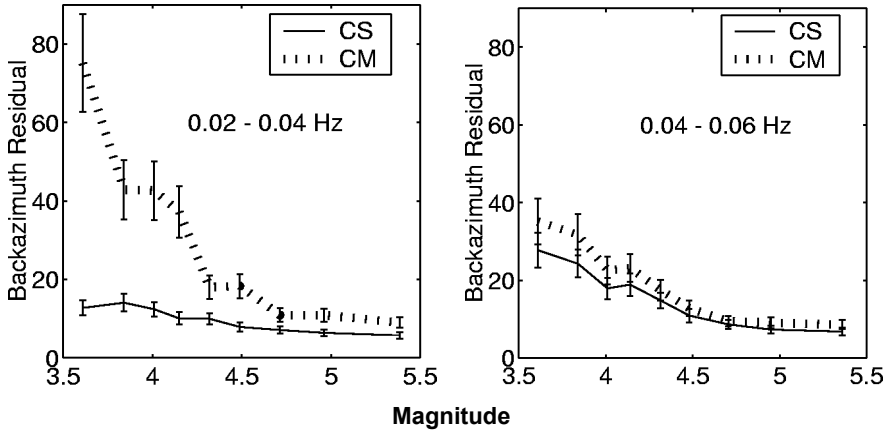

Figure 3. Median ±2 SMAD confidence intervals of backazimuth residuals binned by M_s values for the CM (dotted) and CS_1 algorithm (solid). Each bin has 250 backazimuth residuals. Results at 0.03–0.05 Hz are intermediate between those shown.

The cross correlation of the Hilbert transformed vertical component with the radial predicts the accuracy of the backazimuth estimate. Figure 4 shows backazimuth residuals vs the cross correlation for the best implementation of the CS algorithm applied to data that pass the dispersion test. This ability to predict backazimuth estimate accuracy can aid association with known events. In particular, the strict dispersion criteria for detection at the IDC could be relaxed in cases where the backazimuth is consistent with the theoretical backazimuth and the cross-correlation value is high.

Figure 5 shows the results of the CS method applied to the poorer S/N records that did not pass the dispersion test. This method extracts accurate backazimuth estimates for many of these data, and the more accurate estimates can be

identified by their cross-correlation value. The middle plot shows histograms just for data with a cross-correlation ≥ 0.8, which comprise 14.7% of the data. Their backazimuth residual has a SMAD of 14.8°. The F-statistic of the CM does not provide similar predictive capabilities.

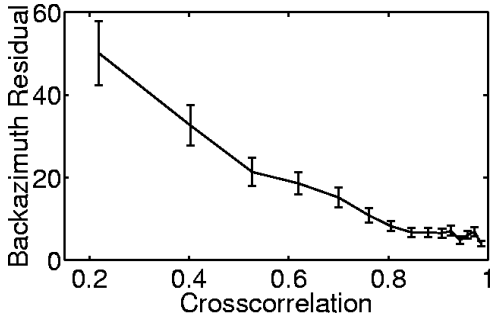

Figure 4: Median backazimuth residuals ±2 SMAD confidence intervals at 0.03–0.05 Hz vs the median cross correlation of the radial and Hilbert transformed vertical Rayleigh waves, for bins of 171 measurements. Results are similar for the other passbands.

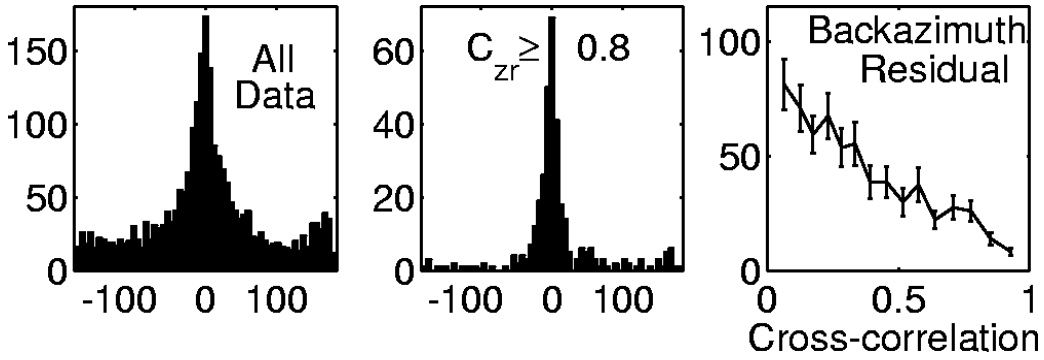

Figure 5. Backazimuth residuals at 0.02–0.04 Hz for the CS algorithm, applied to data not passing the dispersion test. Histograms of backazimuth residuals for all the data (left column) and for the 14.7% of the data with cross correlation ≥ 0.8 (middle). The right-hand plot shows median backazimuth residual ±2 SMAD confidence intervals vs cross correlation, as in Figure 4.

Optimized surface wave amplitude measurements

Surface wave measurements traditionally are accomplished by measuring a time-domain amplitude at a period near 20 seconds and then calculating a surface wave magnitude M_S. This procedure is problematic at regional distances because the surface wave is not well dispersed and a distinct 20-second arrival may not be present. It is possible to measure time-domain amplitudes at higher frequencies with corrections (e.g., Marshall and Basham, 1972), however measurements may be inaccurate due to differences in dispersion caused by differences in earth structure. Stevens and McLaughlin (2001) suggested as an alternative replacing time-domain measurements with a path-corrected spectral magnitude. The path corrected spectral magnitude, $\log M_0$, is calculated by dividing the observed surface wave spectrum by the Green's function for an explosion of unit moment and taking the logarithm of this ratio, averaged over any desired frequency band. Stevens et al. (2003) performed a study to determine the optimum procedures and optimum frequency band for measuring $\log M_0$. This is necessary because there are a number of factors that can affect $\log M_0$, including noise levels, spectral dips and peaks, and the shape of the source spectrum.

The path-corrected spectral magnitude is defined as the logarithm of

$$M_0^{'} = \left| U(\omega, r, \theta) \Big/ \left(\frac{S_1^x(\omega, h_x) S_2(\omega) \exp\left[-\gamma_p(\omega) r\right]}{\sqrt{a_e \sin(r/a_e)}} \right) \right| \qquad (2)$$

where U is the observed surface wave spectrum, S_1^x depends on the source region elastic structure and the explosion source depth, S_2 depends on the receiver-region elastic structure. γ_p is the attenuation coefficient that depends on the attenuation integrated over the path between the source and receiver. a_e is the radius of the earth, and $M_0^{'} = \frac{3\beta^2}{\alpha^2} M_0$ where M_0 is the explosion isotropic moment, defined this way so that the function S_1^x does not depend explicitly on the material properties at the source depth. All of the functions in equation 2 are easily derived from plane-layered earth models, allow the measurement to be regionalized to account for differences in earth structure at the source and receiver, and are due to attenuation along the path.

The advantages of using logM_0 instead of the traditional surface wave magnitude M_s are that logM_0 is insensitive to dispersion, independent of distance, works well at regional distances, and can be regionalized. Regionalized path-corrected spectral magnitudes incorporate geographic variations in source excitation and attenuation. Some limitations are shared by M_s and logM_0 : spectra from earthquakes vary because of source mechanisms and depth, and errors can occur if the measurement is made in a spectral dip or at high frequencies for a deep event (Figure 6). Azimuthal variations in amplitude caused by focal mechanism also affect the amplitudes of both logM_0 and M_s.

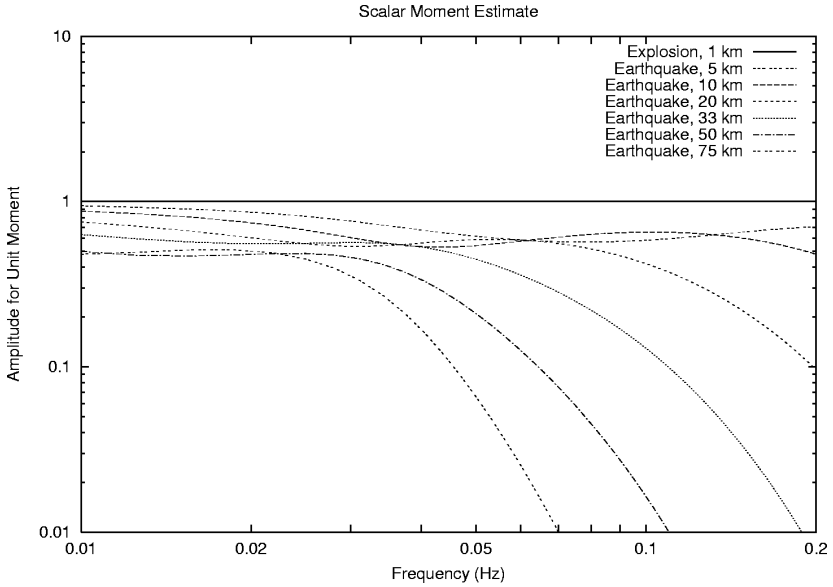

Figure 6. Path-corrected spectra for an explosion and for earthquakes calculated for several depths. The path-corrected explosion spectrum is flat over the entire frequency band (for perfect data and path correction), but the path-corrected earthquake spectrum is flattened and has some variation as a result of source mechanism and source depth.

While a path-corrected spectral magnitude can be measured over any frequency band, it is subject to the following constraints:

1. Earthquake spectra decrease at high frequencies, depending on depth (see Figure 6); therefore, the high end of the frequency band should be low enough that discrimination is not degraded by this effect.
2. At high frequencies, attenuation is higher and the dispersion more variable; therefore the path correction is likely to be less well determined and the signal may be lower than at lower frequencies, particularly at longer distances.
3. Noise increases at low frequency; therefore the low end of the frequency band should be high enough to be above the noise level.

In order to quantify these effects, we created some "path-corrected noise spectra" using path corrections appropriate for the Lop Nor test site. These are simply noise spectra measured at the station that have been divided by an explosion Green's function in the same manner as would be done for a signal. Because the signal spectra are

approximately flat over most of the frequency band, the path-corrected noise spectra are a measure of the minimum path corrected signal that could be measured at each station.

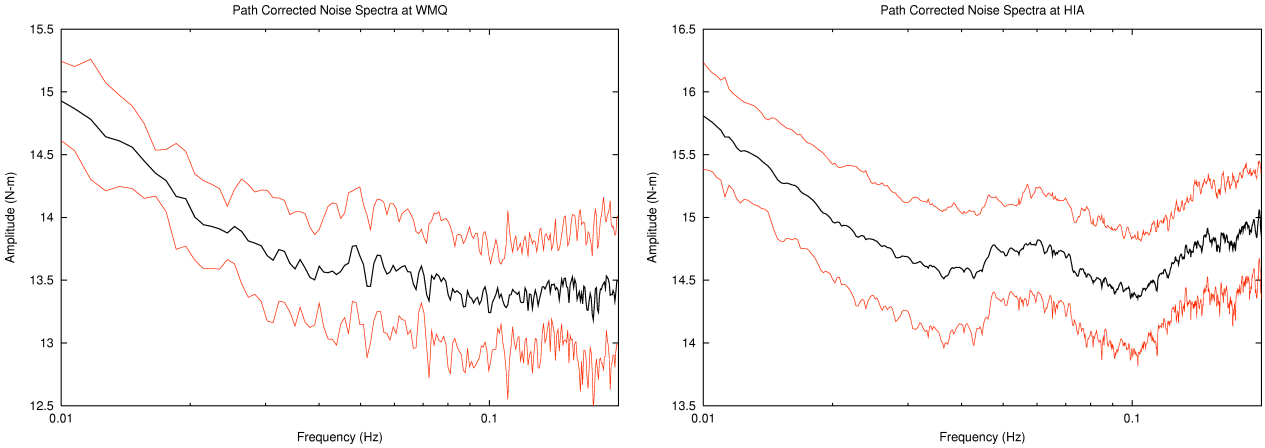

Figure 7. Average path-corrected noise measurement and ±1 standard deviation curves for 13 time segments at WMQ (left) and for 54 time segments at HIA (right). Note that the predicted path-corrected explosion spectrum is flat over this frequency band, and the predicted path-corrected earthquake spectra *decrease* with increasing frequency.

Figure 7 shows the path-corrected noise measurements for two stations: WMQ, located an average of 2 degrees from each event, and HIA, located an average of 27-degrees from each event. At HIA, the noise spectrum has minima at 0.04 and 0.1 Hz, either side of the 0.06 Hz primary microseism peak. Noise amplitudes increase substantially below about 0.04 Hz. Noise levels at WMQ are similar, but are flatter from 0.04 to 0.2 Hz with a less-prominent microseism peak and lower (path corrected) noise at the highest frequencies because of the close distance. Figure 7 shows that there is also considerable variability in the noise level, so that although the average noise level is about 13.5 at WMQ and 14.5 at HIA (corresponding approximately to M_s 1.7 and 2.7, respectively), the minimum spectral magnitude that could be measured may be substantially lower or higher depending on the noise level at the time the measurement is made. These results suggest that in general it is best to measure surface wave spectra at frequencies above 0.03 Hz and below 0.1 Hz. Although noise levels remain fairly low in the 0.1–0.2 Hz frequency band at the closest stations, factors #1 and #2 mentioned above make measurement in this band risky. Based on a number of empirical tests, we recommend measuring surface waves at frequencies between 0.03 and 0.08 Hz for this region. The optimum frequency band may be different in other regions where there are structures that cause large amplitude changes, such as along paths that cross oceanic regions.

Performance of algorithms and analysis of "problem cases"

In many respects surface waves are well behaved and straightforward to model. Two characteristics in particular are helpful (1) because the surface wave always follows a minimum time path, any path other than the great circle path is necessarily longer, which reduces the error in the travel time (in inversions, the main effect of this is to make low-velocity regions appear somewhat smaller than they actually are); and (2) along most continental paths at the regional distances of greatest interest today, and at the periods greater than 10 seconds that are recommended for discrimination, amplitude differences resulting from variations in attenuation are small. Only regions of unusually high attenuation cause significant errors in amplitude predictions along short paths. For most surface wave studies, uncertainties in event location and measurement error are responsible for more of the unmodelable error than actual differences because of complexities in the earth. There are some exceptions to this, however. In cases where surface waves travel along grazing paths near large changes in earth structure, surface waves can be much more complex and difficult to model. Multiple interfering or distinct surface wave arrivals can be observed that take different paths through or around a low-velocity region. The Tarim Basin in western China is a particularly strong example of this effect. In this case, dispersion models can at best predict the dominant surface-wave arrival, and the amplitude may not be predictable without detailed analysis of the data and the earth structure that causes the variations. One technique that we found to help for achieving consistency of measurement and reliability of the inversion is to review the data and order (select) the arrivals so that the dispersion picks change from fast to slow to fast smoothly as the azimuth changes across the basin. Although this doesn't completely resolve the multiple arrival problem, it

selects the arrivals in a manner consistent with waves traveling on a continuous set of paths across the complex earth structure. We plan to investigate this further using numerical modeling of surface waves.

CONCLUSIONS AND RECOMMENDATIONS

The dispersion models developed in this study can be used to find the phase and group velocities between any two points on the earth at any frequency. These models are available to all researchers on request, and have been provided for use in a number of other research projects. The dispersion models depend on dispersion data for accuracy, and so can be improved as more dispersion data become available. We therefore recommend continuation of this iterative process. As more data become available, particularly from regions or in frequency bands currently sparsely covered, we can improve the models and in turn provide these predictions for comparison with and as a starting point for new surface wave studies in regions of interest.

The azimuth estimation algorithm currently used at the International Data Center should be replaced with the Selby/Chael algorithm that was implemented and tested in this project. The procedure can be used together with the dispersion test to reduce the detection threshold for automatic surface wave processing by relaxing the requirements of the dispersion test when the azimuth estimate is consistent with an event hypothesis with a high-correlation value.

The path-corrected spectral magnitude provides a "regional Ms" which has been a long-term goal of this program. The path-corrected spectral magnitude can be measured over any frequency band; however, for discrimination purposes, surface waves should be measured at periods greater than 10 seconds. Periods of 10 seconds and longer can be measured even at very close range, and there is only a small S/N improvement, if any, at shorter periods. Measurement at higher frequencies risks error in discrimination because of the decrease in earthquake spectral amplitude relative to explosions at higher frequencies, particularly for events for which shallow depth is uncertain.

Additional work is needed regarding how to model and invert surface wave amplitude and dispersion in regions of complex earth structure. In particular, surface waves traveling at near-grazing incidence to strong heterogeneities may exhibit amplitude variations not only as a result of focusing/defocusing, but also because of interference of arrivals taking multiple paths through the medium. Similarly, dispersion measurements are complicated by the presence of distinct, multiple arrivals at short periods and interfering arrivals that cannot be separated at longer periods.

ACKNOWLEDGEMENTS

We would like to thank Mike Ritzwoller, Anatoli Levshin and Nikolai Shapiro of the University of Colorado, Bob Herrmann of St. Louis University, and other researchers who have allowed us to use their data in this project.

REFERENCES

Baker, G. Eli and Jeffry L. Stevens (2004), "Backazimuth Estimation Reliability Using Surface Wave Polarization," Geophysical Research Letters, v. 31, L09611, doi:10.1029/2004GL019510.

Bassin, C., G. Laske, and G. Masters (2000), The Current Limits of Resolution for Surface Wave Tomography in North America, *EOS Trans AGU* 81, F897.

Chael, E. (1997), An Automated Rayleigh-Wave Detection Algorithm, *B.S.S.A*., 87, 157-163.

Ekstrom, G., A. M. Dziewonski, G. P. Smith, and W. Su (1996), Elastic and Inelastic Structure Beneath Eurasia, in *Proceedings of the 18th Annual Seismic Research Symposium on Monitoring a Comprehensive Test Ban Treaty, 4-6 September, 1996*, Phillips Laboratory Report PL-TR-96-2153, July, ADA313692, 309-318.

Engdahl, E. R., R. van der Hilst, and R. Buland (1998), Global Teleseismic Earthquake Relocation with Improved Travel Time and Procedures for Depth Determination, *Bull. Seismol. Soc. Am*. 88, 722-743.

Huang, Z., W. Su, Y. Peng, Y. Zheng, and H. Li (2003), Rayleigh Wave Tomography of China and Adjacent Regions. *J. Geophys. Res*. 108(B3), 2073, doi: 10.1029/2001JB001696.

Kennett, B. L. N. E. R. Engdahl, and R. Buland (1995), Constraints on Seismic Velocities in the Earth from Travel Times, *Geophys. J. Int*. 122, 108-124.

Laske, G. and G. Masters (1997), A Global Digital Map of Sediment Thickness, *EOS Trans. AGU* 78, F483.

Laske, G., G. Masters, and C. Reif, Crust 2.0 (2001): A New Global Crustal Model at 2x2 Degrees, http://mahi.ucsd.edu/Gabi/rem.html.

Levshin, Anatoli L., Jeffry L. Stevens, Michael H. Ritzwoller, David A. Adams, and G. Eli Baker (2003), "Improvement of Detection and Discrimination Using Short Period (7s-15s) Surface Waves in W. China, N. India, Pakistan and Environs," Final report submitted to Defense Threat Reduction Agency, SAIC Report No. 03/2008, CU Project No. 1532378, April.

Levshin, A. L., M. H. Ritzwoller, and S. S. Smith (1996), "Group Velocity Variations Across Eurasia," in *Proceedings of the 18th Annual Seismic Research Symposium on Monitoring A Comprehensive Test Ban Treaty,* Phillips Laboratory Report PL-TR-96-2153.

Marshall, P. D. and P. W. Basham (1972), Discrimination Between Earthquakes and Underground Nuclear Explosions Employing an Improved Ms Scale, *Geophys. J. R. astr. Soc*. 28, 431-458.

Mitchell, B. J., L. Cong and J. Xie, (1996), "Seismic Attenuation Studies in the Middle East and Southern Asia", St. Louis University Scientific Report No. 1, PL-TR-96-2154, ADA317387.

Ritzwoller, M. H., A. L. Levshin, L. I. Ratnikova, and D. M. Tremblay (1996), "High Resolution Group Velocity Variations Across Central Asia, "*Proceedings of the 18th Annual Seismic Research Symposium on Monitoring A Comprehensive Test Ban Treaty"*.

Ritzwoller, M.H., O.Y Vdovin, and A.L. Levshin (1999), "Surface Wave Dispersion Across Antarctica: A First Look", Antarctic J. U.S., in press.

Selby, N.D. (2001), Association of Rayleigh Waves Using Backazimuth Measurements: Application to Test Ban Verification. *Bull. Seism. Soc. Am*., 91, 580-593.

Smart, E. (1978), A three-component, single-station, maximum-likelihood surface wave processor, *Geotech Report No*. SDAC-TR-77-14.

Stevens, J. L. (1986), "Estimation of Scalar Moments From Explosion-Generated Surface Waves," *Bull. Seism. Soc. Am.*, v. 76, pp. 123-151.

Stevens, J. L. and S. M. Day (1985), "The Physical Basis of the mb:Ms and Variable Frequency Magnitude Methods for Earthquake/Explosion Discrimination," *Journal of Geophysical Research*, v. 90, pp. 3009-3020.

Stevens, J. L. and D.A. Adams (2000), Improved Surface Wave Detection and Measurement Using Phase-Matched Filtering and Improved Regionalized Models, in *Proceedings of the 22nd Annual DOD/DOE Seismic Research Symposium: Planning for Verification of and Compliance with the Comprehensive Nuclear-Test-Ban Treaty (CTBT), 12-15 September 2000*, 145-154.

Stevens, J. L., D. A. Adams, and E. Baker (2001), *Surface Wave Detection and Measurement Using a One Degree Global Dispersion Grid*, SAIC Final Report to Defense Threat Reduction Agency, SAIC-01/1084, December.

Stevens, J. L. and K. L. McLaughlin (1996), "Regionalized Maximum Likelihood Surface Wave Analysis," Maxwell Technologies Technical Report PL-TR-96-2273, SSS-DTR-96-15562, September.

Stevens, J. L., and K. L. McLaughlin (1988), "Analysis of surface waves from the Novaya Zemlya, Mururoa, and Amchitka test sites, and maximum likelihood estimation of scalar moments from earthquakes and explosions," S-CUBED technical report SSS-TR-89-9953, September.

Stevens, J. L. and K. L. McLaughlin (2001), Optimization of Surface Wave Identification and Measurement, *Pure Appl. Geophs.* 158, 1547-1582.

Stevens, J. L., D. A. Adams, and M. G. Eneva (2003), "Improved Surface Wave Dispersion Models and Amplitude Measurements," *Proceedings of the 25th Annual Seismic Research Review - Nuclear Explosion Monitoring: Building the Knowledge Base*, Tucson, AZ, 23-25 September, 2003.

Vdovin, O. Y., J. A. Rial, M. H. Ritzwoller, and A. L. Levshin (1999), "Group-velocity tomography of South America and the surrounding oceans", *Geophys. J. Int.*, 136, 324-330.

Yang, X., S. R. Taylor, H. J. Patton, M. Maceira, and A. A. Velasco (2002), Evaluation of Intermediate-Period (10- to 30-sec) Rayleigh-Wave Group Velocity Maps for Central Asia, in *Proceedings of the24th Seismic Research Review - Nuclear Explosion Monitoring: Innovation and Integration,* 17-19 September 2002*,* 609-617.